Sweety, salty, sour, and romantic biochar-supported ZnO

Bhakta, Arvind K.; Tang, Mengqi; Snoussi, Youssef; Khalil, Ahmed M.; Mascarenhas, Ronald J.; Mekhalif, Zineb; Abderrabba, Manef; Ammar, Souad; Chehimi, Mohamed M.

Published in:
Emergent Materials

DOI:
10.1007/s42247-023-00599-5

Publication date:
2023

Document Version
Publisher's PDF, also known as Version of record

Emergent Materials
https://doi.org/10.1007/s42247-023-00599-5

ORIGINAL ARTICLE

Sweety, *salty*, *sour*, and *romantic* biochar-supported ZnO: highly active composite catalysts for environmental remediation

Arvind K. Bhakta[1,2] · Mengqi Tang[1] · Youssef Snoussi[1] · Ahmed M. Khalil[3] · Ronald J. Mascarenhas[2] · Zineb Mekhalif[4] · Manef Abderrabba[5] · Souad Ammar[1] · Mohamed M. Chehimi[1]

Received: 20 July 2023 / Accepted: 22 November 2023

Abstract
The present work focuses on valorizing the various biochar supports of nano-catalysts and investigates the effect of the type of the initial biomass on the deposition and salient physico-chemical features of the zinc oxide (ZnO) nanoparticles. In this regard, we have used four different biomasses, namely, sugarcane bagasse (*Saccharum officinarum*), algae (*Phaeophyta*), mandarin orange peels (*Citrus reticulata*), and China rose petals (*Rosa chinensis*) as sources of biochar. Their wet impregnation with zinc acetate was followed by pyrolysis at 500 °C. It led to biochar (nicknamed "sweety," "salty," "sour," and "romantic" biochar, respectively) loaded with very well dispersed, 20–360 nm-sized (mostly) ZnO nanoparticles. Interestingly, depending on the type of biomass used, the size, shape (quartz-like, semi-spherical, spherical, semi-cauliflower, needle or rod-like), and degree of crystallinity of ZnO nanoparticles (hexagonal crystal system) vary, in spite of all other synthesis parameters being similar. Nanoparticle-induced graphitization and crystallization of biochar have been also observed by Raman spectroscopy. The malachite green dye mineralization efficiency in the presence of H_2O_2 and different biochar-supported ZnO nanocatalysts was 15.1%, 46.3%, 99.9%, 67.9%, and 66.4% for H_2O_2, china rose petals, algae, mandarin peels, and sugarcane bagasse-supported ZnO catalyst in the presence of H_2O_2, respectively. Malachite green removal fits in very well with a pseudo-first-order kinetic model with $R^2 = 0.9701$ (at algae biochar-ZnO). 6.6 times enhancement in the mineralization efficiency is observed as compared to just H_2O_2. The recyclability test of algae biochar impregnated with ZnO after 5 cycles indicates the mineralization efficiency levels up to 81.4%. Beyond these scientific results, this work is based on the principle of biomass waste valorization for sustainable development and circular economy, on the one hand, and addresses the UN Sustainable Development Goals 6, 13, and 14, on the other hand. It is also very clear that biochar is the *new romance* in the field of materials science and for sustainable future.

Keywords Trash-to-treasure, Environmental remediation · *Rosa chinensis* · *Saccharum officinarum* · *Citrus reticulata* · Phaeophyta · Sustainability

✉ Arvind K. Bhakta
arvind-kumar.bhakta@u-paris.fr

✉ Mohamed M. Chehimi
mohamed.chehimi@cnrs.fr

1 Université Paris Cité, CNRS, ITODYS (UMR 7086), 75013 Paris, France

2 Department of Chemistry, St. Joseph's University, 560 027 Bengaluru, India

3 Photochemistry Department, National Research Centre, Dokki 12622, Giza, Egypt

4 CES, NISM, University of Namur, B-5000 Namur, Belgium

5 Laboratory of Materials Molecules and Applications, Preparatory Institute for Scientific and Technical Studies, University of Carthage, 2070 Carthage, Tunisia

1 Introduction

In the current scenario of the world, humanity is facing many challenges such as new disease outbreaks (novel coronavirus and monkeypox) [1, 2], inflation[3], poverty [4], climate change [5], water and air pollution [6, 7], and war and food crisis [8]. Throughout the globe, synthetic organic dyes are manufactured > 10^6 t per year commercially. They are utilized for various purposes such as cosmetics, textiles, food, tannery, and pharmaceutical industry [9, 10]. One such dye is malachite green (MG). It is stable and stays for longer duration in environment, results in their entry into food chain. They are mutagenic, carcinogenic, and genotoxic [11–14]. It becomes essential to shift our focus towards the

Published online: 13 December 2023

concept of water treatment, sustainable development [15], circular economy [16, 17], and waste to wealth or trash to treasure [18]. This is the reason why efforts have already been started towards this concept by working on biomass waste valorization [19].

One way to valorize biomass is to produce biochar [20]. Biomass-derived carbon produced via pyrolysis is termed as biochar [21, 22]. They are well known for their unique physical (surface area, surface charge, high porosity, and water holding capacity), chemical (cation exchange capacity, carbon sequestration, nutrient exchange site, high pH, and surface functionalities: –COOH, –OH, –R–OH, and C = O), and agronomic properties (salinity and nutrients) [23–25]. They are employed in various applications [26] such as pesticide decontamination [27], soil amendment [28, 29], oil removal [30], anti-kinetoplastid agents [31], dye degradation [32, 33], lipase immobilization [34], drugs degradation [35, 36], personal care products removal [37], NH_3 sorption [38], hydrogen production [25], reinforcing fillers [39], combustible briquettes [40], biorefinery [41], fertilizers [42], hydrocarbon removal [43], to mention but a few. Biochar also acts as a source for synthesizing other carbon allotropes such as graphene oxide [44].

Biochar activation can be achieved through different treatments [45, 46] such as chemical activation (HCl, H_2SO_4, NaOH, $ZnCl_2$, KOH, K_2CO_3, citric acid) [47, 48] and physical activation (electrochemical modification, microwave, plasma treatment, and ultrasonication irradiation, gaseous such as steam, ozone, and CO_2) [49]. As biochar is a very good substrate to disperse nanocatalyst, it is one of the potential candidates to host zinc oxide II-IV (ZnO), which is an n-type semiconductor. ZnO has high excitation energy (60 meV) at ambient temperature and possess wide range band gap (3.37 eV). They are thermally and chemically stable, anti-microbial, cost-effective, exhibit optical properties of photoluminescence [50] like some organic compound [51], eco-friendly, easy to use, and bio-compatible [52–54]. They can be synthesized in different sizes, shapes [55], and multifunctionalities [56]. These unique properties make it one of the most favorable catalysts among metal oxides to be utilized in the field of dye degradation [57, 58].

This biochar/ZnO composite can be one of the best fits for water decontamination because of the following reasons: (1) both biochar and ZnO are economic, (2) ZnO is photocatalyst [9, 59, 60], and (3) due to electron conductive nature of biochar, it can reduce the e-/h recombination during photocatalysis [61]. There are two major ways to depollute water: either adsorption [62] or degradation /mineralization. In adsorption, the fate of an adsorbate is not so clear. In degradation, sometimes the partially degraded product can be toxic. Hence, mineralization is one of the best ways to treat wastewater pollutants. In this scenario, advanced oxidation process (AOP) [32, 63, 64] is very popular for the removal of toxic and persistent organic pollutants [65]. Their efficiency is enhanced by heterogeneous catalyst. Preparation of catalyst and treatment of pollutant at industrial scale as well new emerging pollutant [66] are still challenging. Thus, need for cost-effective and efficient catalysts is still there for water decontamination. It rests on the utilization of efficient photocatalysts that are favored to be dispersed over a plethora of supports. Biochar@ZnO materials are the subject of current and timely investigations in the domain of environmental chemistry. Herein, our main objective is to valorize various biochar supports of nanocatalysts, and investigate the effect of type of the initial biomass on the deposition and salient physico-chemical features of the zinc oxide (ZnO) nanoparticles.

In the present work, we have utilized four different biomasses, namely, algae, China rose petals, sugarcane bagasse, and mandarin orange peels. Their biochars act as active supports to host ZnO nanophotocatalyst. The selection criteria of biomass were based on considering different group of biomasses. Sugarcane bagasse represents the industrial waste, algae is a third-generation biomass [67] and available in plenty, and rose petals and mandarin are the biomass produced in our day today life. Also, they represent biomass with different porosity and hydrophobicity/hydrophilicity.

Depending on the chosen biomass, the size and morphology of ZnO vary. They are successfully applied in complete mineralization of MG dye. Though, in the literature, biochar@ZnO have already been used for the pollutant removal, for example, pecan nutshell biochar-ZnO for acid red 97 removal [68], hemp stem biochar/ZnO for methylene blue (MB) degradation [69], *Calotropis gigantea* biochar-ZnO for ciprofloxacin [70], and maize biochar-ZnO for organic and inorganic pollutants [71]. Mostly, single biomass had been considered as support for ZnO. Some have considered two different biomasses (brewed coffee and chitosan) but without obtaining any differences in the ZnO characteristics [72]. In review papers, general aspects are covered and performances of individual biochar@ZnO are compiled in synoptic tables [73–75]. Given the countless number of biomasses available for making biochar photocatalyst, we reasoned it is worth to investigate the physicochemical characteristics and compare the performances of various biochar@ZnO catalysts obtained by conversion of four different zinc acetate impregnated biomasses. To the best of our knowledge, no paper has tackled the effect of biomass/agrowaste nature on the properties and performances of ZnO in the same investigation, hence our motivation for this contribution. The results obtained clearly show that the effect of nature of biomass on ZnO nanoparticle growth synthesized in the same condition is quite impressive and unique. This work also takes into account the United Nations Sustainable Development Goals 6, 13, and 14 [76]. The cost-effectiveness in terms of converting trash to treasure is one of the advantages of this work.

2 Materials and methods

2.1 Chemicals

Malachite green oxalate salt and zinc acetate (99.99%) were obtained from Sigma and Aldrich, respectively. Double-distilled water was used to prepare all aqueous solution.

H_2O_2 (30%) was received from Merck. Sugarcane (*Saccharum officinarum* L.) was cultivated in Minya Governorate, Upper Egypt, and mandarin orange (*Citrus Reticulata Blanco*) was cropped in Ismailia Governorate, Egypt. ETS Laurent Mace (Huitres Creuses de Normandie, F-50560 Gouville-Sur-Mer) has provided algae samples.

2.2 Apparatus

Cary 4000 UV–vis spectrophotometer (SpectraLab Scientific Inc., Markham, Ontario, Canada) was utilized to do kinetic studies in the UV–vis range. FESEM study was carried out using GeminiSEM 360. Accelerating voltage and emission current were maintained at 5 kV and 30 µA, respectively. Sample preparation step involves drop casting of dispersed biochar in ethanol on silica plate, which is fixed on sample holder via carbon tape. Horiba HR 800 spectrometer (Kyoto, Japan) was used to perform Raman study. He–Ne laser beam wavelength was set to 633 nm. The range of the spectra acquired was 800 to 2700 cm^{-1} region. X'Pert PRO PANalytical instrument (Cambridge, UK) was used for XRD characterization. This instrument was maintained at operating voltage = 40 kV, and tube current were kept = 40 mA. XPS was performed on a Thermo-Scientific K Alpha + instrument with pass energy = 200 and 80 eV for survey scan and high-resolution spectra, respectively.

2.3 Synthesis of ZnO-coated biochar

2.3.1 Biomass powder preparation

Sugarcane bagasse powder and mandarin orange peel powder were designated as SB and MOP, respectively. The leftover dried China rose flower petals were plucked, washed with two times with tap water, followed by two times with distilled water. Then, they were dried at 60 °C for 66 h. Furthermore, they were ground in coffee mill for 2 min. This is labeled as CRP. Algae biomass was washed two times with tap water and two times with distilled water, dried in air for a week then in oven at 60 °C overnight. It was then ground in coffee mill for 2 min. This is labeled as A.

2.3.2 Impregnation of biomass with zinc acetate

A wet impregnation technique was used to impregnate the biomass [77]. The amount of different biomass and zinc acetate used (1 mmol of zinc acetate/1 g of biomass) are shown in Table 1. After wet impregnation, all the samples were dried overnight in oven at 60 °C and ground using mortar and pestle.

2.3.3 Preparation of ZnO-coated biochar

Zinc acetate-impregnated different biomass samples were pyrolyzed to obtain ZnO-coated biochar as shown in Fig. 1. Pyrolysis furnace (Carbolite Gero) was maintained at type of method: P10 KOH free, N_2 gas flow rate 1 L/min, ramp 20 °C/min, temperature 500 °C, residence time 1 h, and cooling time 1 h. The percentage yields are reported in Table 1.

A pyrolysis temperature of 500 °C is preferred to make biochar because from the literature, It is found that at this

Table 1 Type of the used biomass, impregnated and corresponding biochar with yield %

Type of samples and designation (before pyrolysis)	Weight (g) before pyrolysis	Sample designation after pyrolysis	Weight (g) after pyrolysis	Yield %
A: Algae powder	1.0009	AB (salty biochar)	0.3420	34.2%
A@ZA: 1.004 g of algae biomass powder was mixed with solution (10 mL water + 183.48 mg zinc acetate), dried in oven for 60 °C overnight, and ground.	1.0908	AB@ZnO	0.4316	43.1%
CRP: China rose petals powder	1.0026	CRPB (romantic biochar)	0.3018	30.1%
CRP@ZA: 1.0006 g of China rose petal powder was mixed with 10 mL solution of 183.5 mg of zinc acetate, dried in oven overnight at 60 °C and ground.	1.0352	CRPB@ZnO	0.3659	35.4%
MOP: mandarin orange peel powder	1.0234	MOPB (sour biochar)	0.2913	28.5%
MOP@ZA: 1.0019 g mandarin orange peels powder were mixed with solution containing 10 mL of water and 183.5 mg zinc acetate, dried in oven for 60 °C overnight, and ground.	0.9727	MOPB@ZnO	0.3470	35.7%
SB: sugarcane bagasse powder	1.0065	SBB (sweety biochar)	0.2265	22.5%
SB@ZA: 1.0000 g sugarcane bagasse powder was mixed with zinc acetate solution (10 mL water + 183.5 mg zinc acetate), dried in oven for 60 °C overnight and ground.	1.0523	SBB@ZnO	0.3174	30.2%

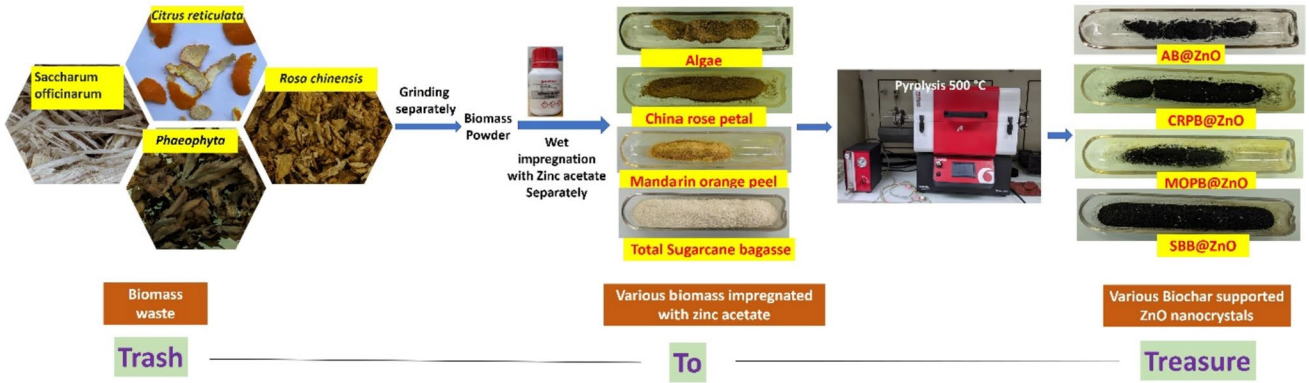

Fig. 1 Schematic representation of different biomass impregnated with zinc acetate and corresponding ZnO-coated biochar

temperature, per- and polyfluoroalkyl substances (PFASs) have been removed partially (more than 97%) or completely depending on the used sample [78]. Thus, to avoid PFAS in biochar, a moderate temperature pyrolysis is preferred [79].

2.4 Mineralization of malachite green

One milligram of catalyst was added into the 10 mL of 50 ppm malachite green aqueous solution. Further, 100 µL H_2O_2 was added and stirred for 60 min. Thereafter, UV–vis measurement has been carried out. This experiment was performed up to 60 min for studying the kinetics (0, 15, 22, 30, 45, and 60 min). The reusability of the catalyst was checked for 5 cycles. Firstly, 10 mL of 50 ppm MG solution was added into beaker followed by 1 mg catalyst and 100 µL H_2O_2 for 60 min. After that, the same amount of solution (MG + H_2O_2) was added in the same beaker. This process was repeated until 5 cycles are completed. Note: Before conducting all UV–vis measurements (for kinetics and reusability test), filtrate has been diluted by adding 1 mL of filtrate in 3 mL of water.

3 Results and discussions

3.1 Surface morphology

Surface morphology of the different biochars coated with ZnO nanoparticles were studied using FESEM technique (Figs. 2 and 3). The global view of AB@ZnO FESEM micrographs is shown in Fig. 2a. Biochar appears as a coral reef-like structure which is coated with tiny ZnO particles. Furthermore, high-resolution images show bimodal distribution of ZnO nanoparticles (Fig. 3). There are quartz-like nanoparticles (Fig. 3a) formed in the cavities of biochar. The side edge of biochar has an appearance-like ribs possessing semi-spherical particles (Fig. 3b). The particle sizes are less than 100 nm.

FESEM images of CRPB@ZnO (Fig. 2b) show smooth biochar surface with more or less spherical embedded particles (Fig. 3c). In contrast, the biochar obtained from mandarin peels appears very rough (Fig. 2c) and ZnO particles look like pebbles (Fig. 3d).

Interestingly, again, sugarcane bagasse biochar coated with ZnO shows bimodal distribution but entirely different morphology of ZnO nanoparticles. This biochar appears like leaflet (Fig. 2d). There is semi-cauliflower-like nanoparticles (Fig. 3e), and rod or needle-like nanoparticle (Fig. 2f) was observed

As it can be clearly seen (Table 2), all the samples have varieties of ZnO shapes and sizes in spite of their preparations in similar condition. These differences can be attributed to the different chemical composition of biomass in terms of cellulose, lignin, hemicellulose, extractives and other organic and inorganic minerals. Thus, there are two important parameters seem to influence the shape and dispersion of ZnO NPs: the total percentage of lignocellulosic matter and the initial (hemicellulose + lignin)/cellulose ratio. Also, porosity and hydrophobicity/hydrophilicity of biomass matter in this regard. There are two major possibility via a biochar host the nanoparticle: (a) it surrounds the nanoparticles (entangled) and (b) the functional group present on the biochar anchors the nanoparticles [81]. The difference texture and porosity could lead to difference area which could be probed by the BET surface area measurements [82].

3.2 Crystalline structure and elemental composition

The XRD patterns of the different biochars@ZnO are reported in the Fig. 4. In the sample AB@ZnO (Fig. 4), the peak at $2\Theta = 37.0°$, 40.1°, 42.3°, 55.7°, 66.7°, 74.4°, and 78.9° were due the planes (010), (002), (011), (012), (110), (013), and

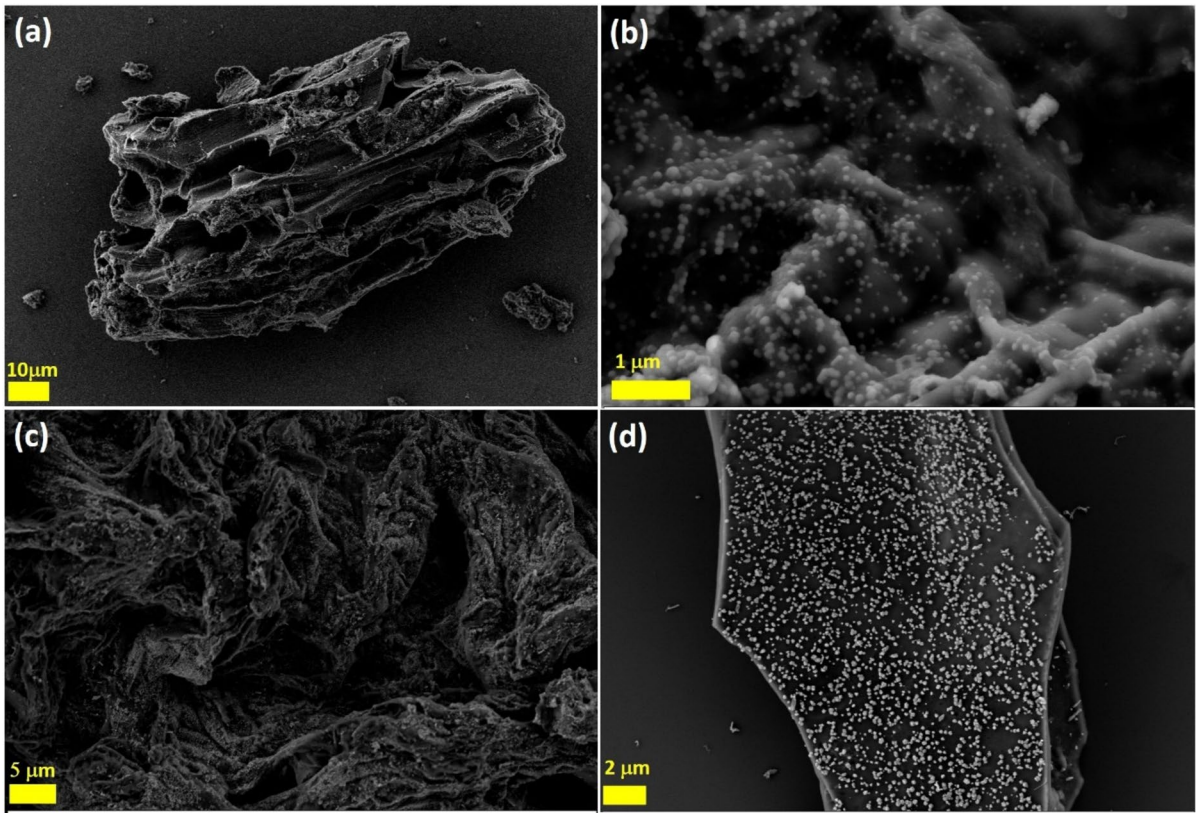

Fig. 2 FESEM images of **a** AB@ZnO, **b** CRPB@ZnO, **c** MOPB@ZnO, and **d** SBB@ZnO

(020), respectively. This is a clear indication of zincite mineral with chemical formula O_1Zn_1 having hexagonal crystal system [83]. The structures of MOPB@ZnO [84], SBB@ZnO [84], and CRPB@ZnO [85] also fall in this category.

The elemental composition of the different biochar samples was studied by XPS, and the data were treated by Avantage software. The atomic composition % is reported in Table 3. It is very clear that the pristine biochar contains Zn, S, N, C, O, Si, Ca, Na, Mg, and Cl (Table 3). In general, in the impregnation of ZnO nanoparticles, the amount of carbon decreases and Zn and O increases. There is an exception observed in the case of algae biochar where it has already good amount of Zn. If we remove the contribution 3.20% from 18.54% (sample AB), we will end up getting 15.34% O, which fullfils the trend of increase in oxygen after ZnO impregnation. Though there is a presence of Na and Cl, it does not have any adverse effect on catalytic activity of AB@ZnO. Sulfate S2p for AB and AB@ZnO could be due to fucan [86]. The modified Auger parameter of biochar@ZnO is at 2010.2 eV, which is in accordance with the literature confirming the zinc in ZnO state [87]. The high-resolution $Zn2p_{3/2}$ and ZnLMM spectra of four biochar@ZnO samples are reported in Fig. 4e and f, respectively.

3.3 Raman study

The Raman characterization was performed to test the quality of biochar samples besides the degree of graphitization and crystallization [88, 89]. The Raman peak fitting (Fig. 5) shows mostly the 6 components as follows: S_L (hydrogen circulation along periphery), *S* (alky-alkyl ether), *D* (defects and heteroatoms), *V* (sp2 carbon), *G* (degree of graphitization), and G_L (carbonyl function) [90]. *D*/G ratio (Fig. 6) has decreased after ZnO impregnation except for MOPB sample, showing that the nanoparticles induced graphitization which is in accordance with literature [91]. This anamoly can be attributed to the different chemical composition and porosity [92].

3.4 Dye mineralization

The application of the four synthesized catalysts is demonstrated in the mineralization of a model pollutant MG dye. The 50 ppm of MG dye treated with 1 mg catalyst in the presence of H_2O_2 resulted in complete mineralization for MG dye in 60 min. Figure 7a demonstrates the UV–vis spectrum of the initial MG dye besides its treatment with just H_2O_2 and in the presence of different catalysts (MOPB@ZnO, SBB@

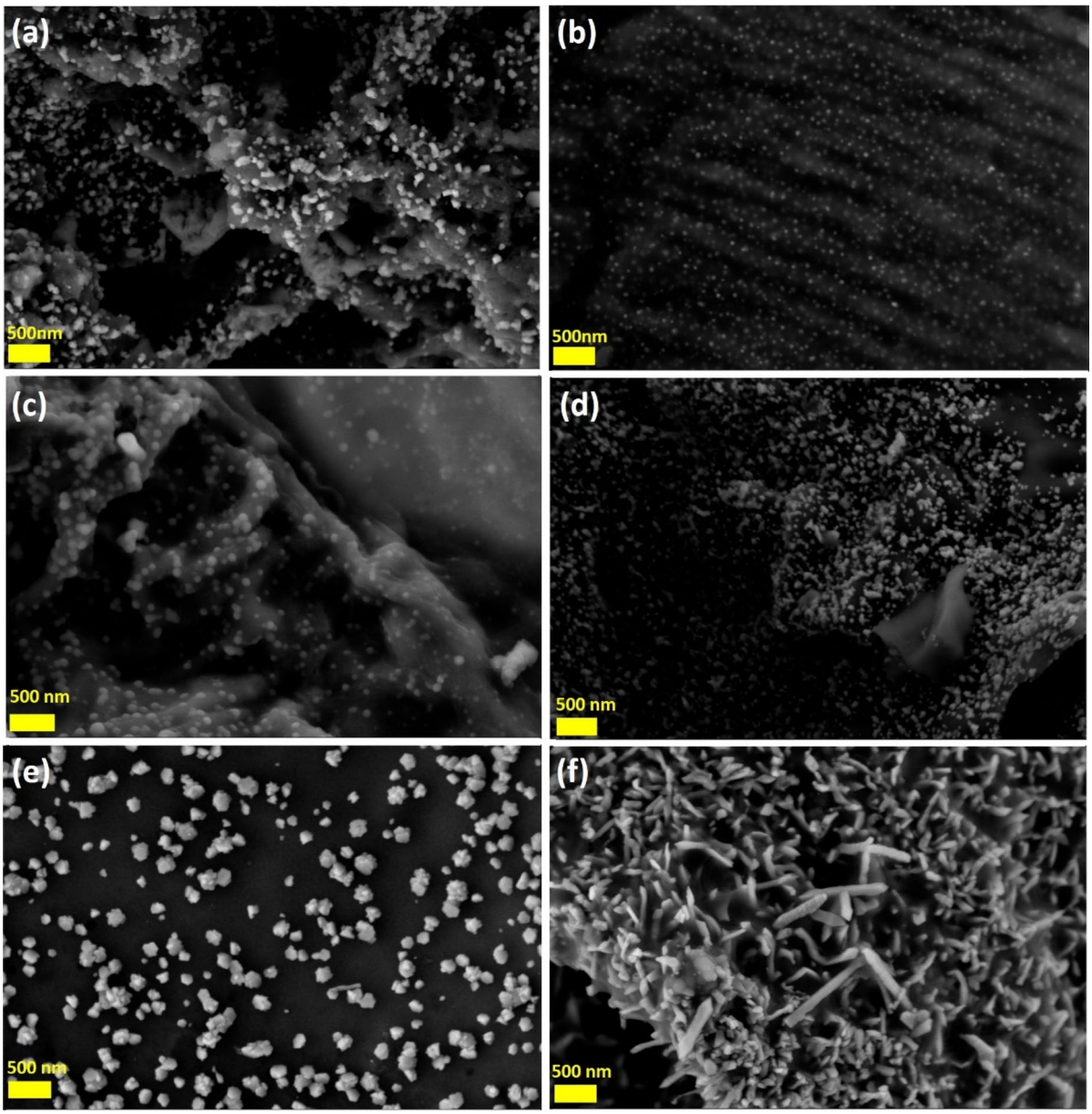

Fig. 3 FESEM images of **a**, **b** AB@ZnO, **c** CRPB@ZnO, **d** MOPB@ZnO, and **e**, **f** SBB@ZnO

Table 2 Cellulose, hemicelluloses, and lignin composition of different biomass with corresponding biochar shape and size of impregnated ZnO nanoparticles

	Cellulose	Hemi-cellulose	Lignin	Shape of biochar	Shape and size (nm) of ZnO
AB@ZnO	*	*	*	Coral reef	Bimodal distribution, quartz (20–200 nm approx.) andsemi-spherical NPs (20–85 approx.)
CRPB@ZnO	NA	NA	NA	Flower or octopus	Spherical particles (25–230 nm approx.)
SBB@ZnO	31.16	25.28	5.35	Leaflet	Cauliflower/semi-cauliflower-like NPs (70–360 nm) and rod or needle-like NPs (80–1190 nm in length and max. width is 150 nm approx.)
MOPB	3.32	5.74	5.7	Porous mountain or honeycomb	Pebbles (15–170 nm)

*Algae (cellulose = 4.6, hemicelluloses = 6.1, and lignin = 19) [80]

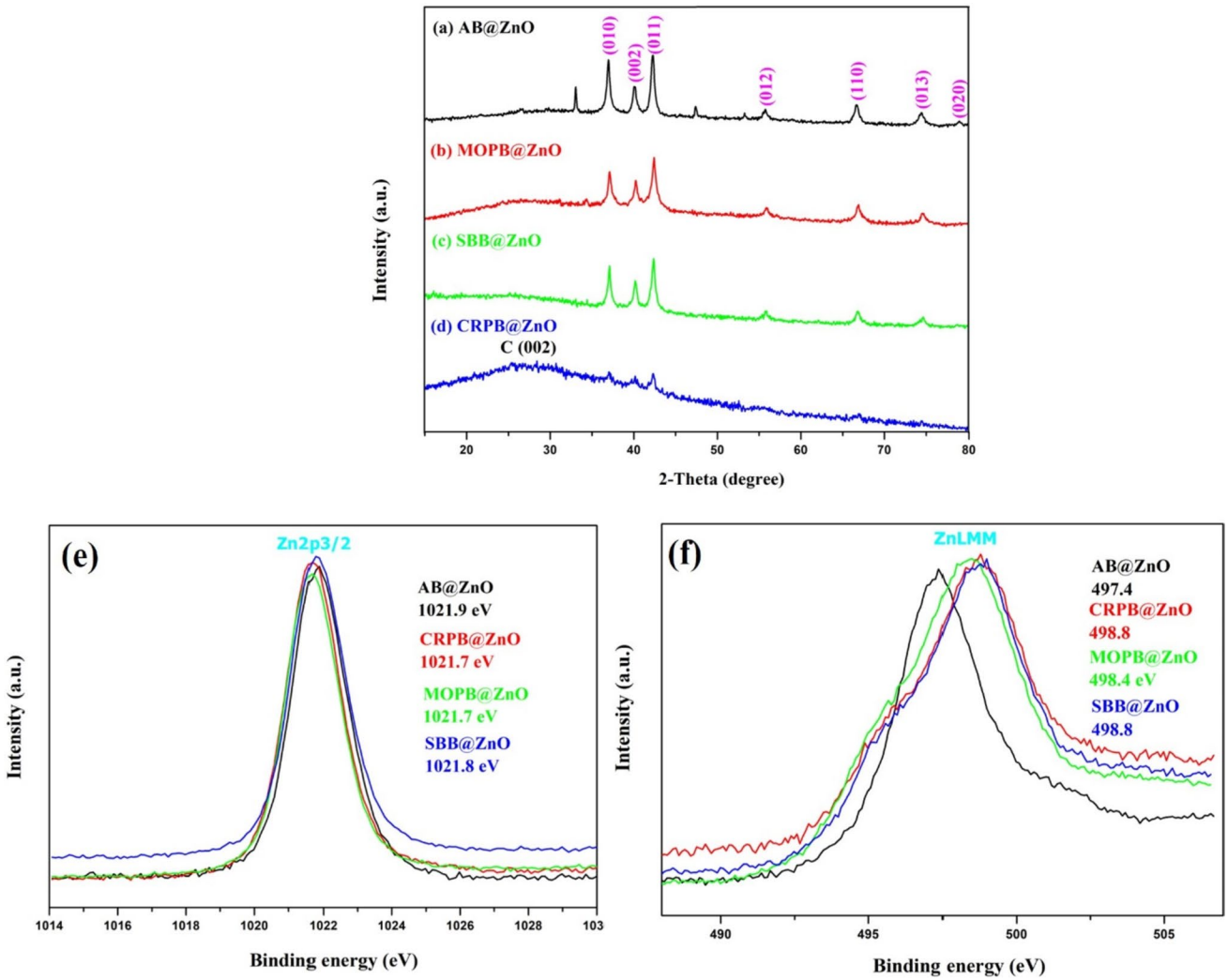

Fig. 4 XRD patterns of **a** AB@ZnO, **b** MOPB@ZnO, **c** SBB@ZnO, and **d** CRPB@ZnO. **e** $Zn2p_{3/2}$ and **f** ZnLMM high-resolution XPS spectra of four biochar@ZnO samples

Table 3 XPS atomic % composition of different biochar and biochar@ZnO samples

Samples	% Zn	% S	% N	% C	% O	% Si	% Ca	% Na	% Mg	% Cl
AB	3.20	1.12	1.00	68.73	18.54	0.35	1.63	2.10	0.99	2.34
AB@ZnO	5.93	0.82	0.92	67.27	17.56	0.34	1.33	2.49	0.93	2.40
CRPB	0.44	0.11	2.35	82.88	11.75	1.70	0.40	0.09	0.19	0.07
CRPB@ZnO	4.71	0.20	1.62	76.25	15.63	0.47	0.29	0.26	0.28	0.28
MOPB	0.09	0.11	1.63	83.39	12.77	0.56	0.75	0.28	0.18	0.24
MOPB@ZnO	9.19	0.13	1.68	71.44	15.23	0.73	0.76	0.37	0.20	0.27
SBB	0.47	0.21	0.99	85.07	11.47	0.97	0.38	0.14	0.20	0.09
SBB@ZnO	7.08	0.16	0.60	73.34	15.64	2.41	0.19	0.22	0.17	0.19

ZnO, CRPB@ZnO, and AB@ZnO). The corresponding mineralization efficiency is plotted in the form of a histogram (Fig. 7b). It is observed that MG dye mineralization occurs in the presence of H_2O_2 and CRPB@ZnO, AB@ZnO, MOPB@ZnO, and SBB@ZnO with the efficiencies of 46.3%, 99.9%, 67.9%, and 66.4%, respectively. On the contrary, mineralization efficiency leveled off at 15.1% in the presence of just hydrogen peroxide. Thus, increasing order of MG dye efficiency follows the following pattern: CRPB@ZnO < SBB@ZnO < MOPB@ZnO < AB@ZnO. MG removal fits in very

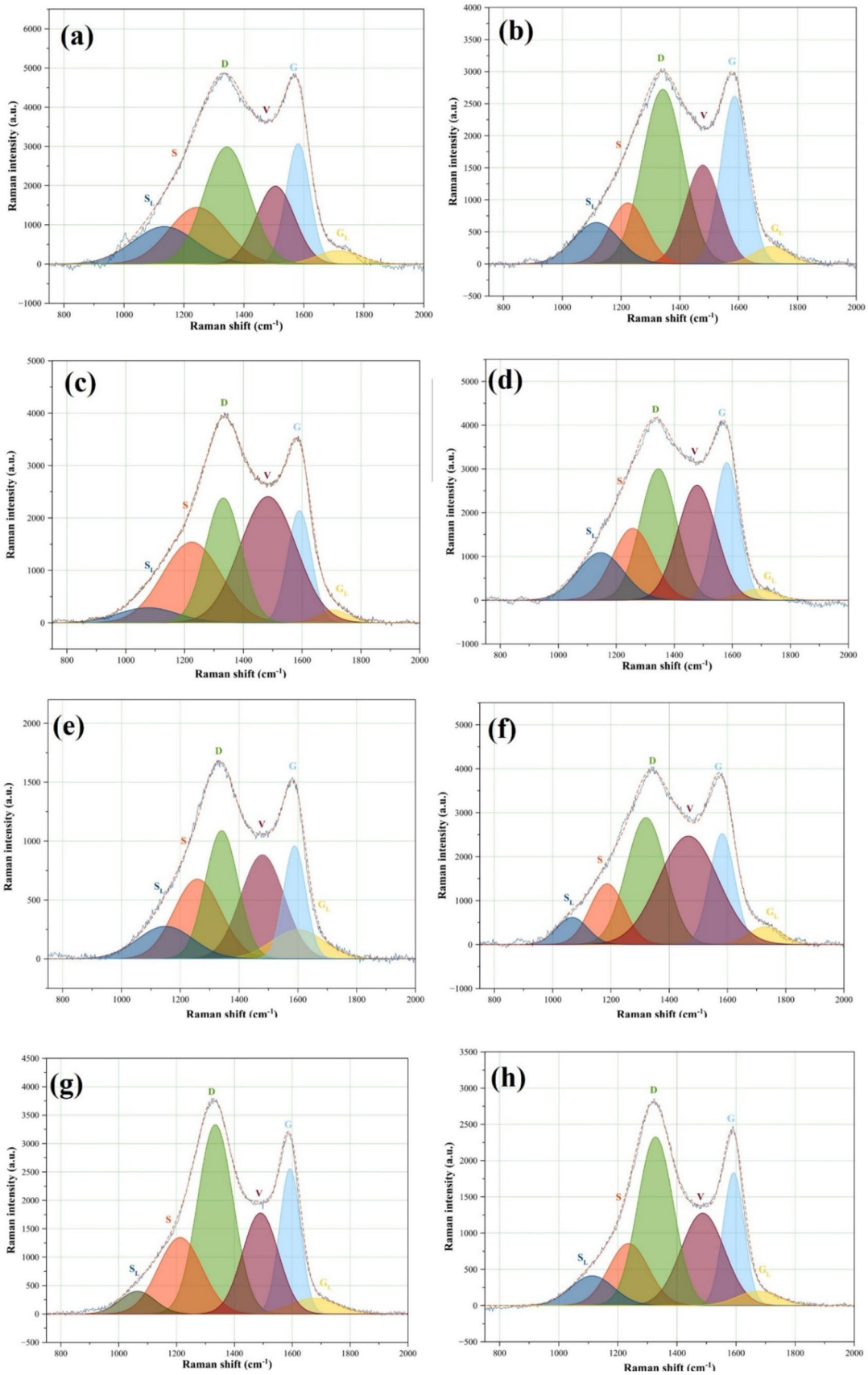

Fig. 5 Raman spectra peak fitting of **a** AB, **b** AB@ZnO, **c** CRPB, **d** CRPB@ZnO, **e** MOPB, **f** MOPB@ZnO, **g** SBB, and **h** SBB@ZnO

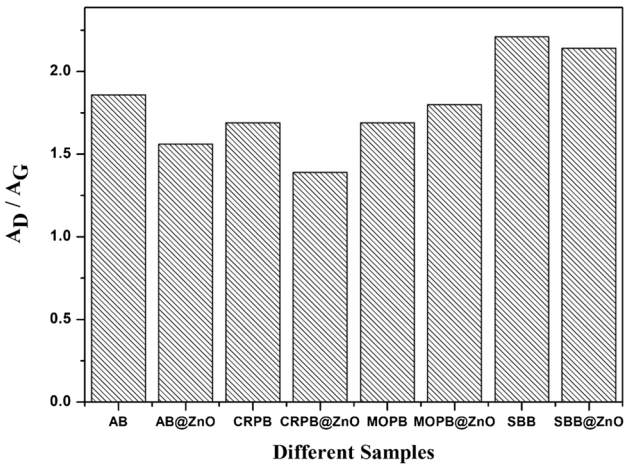

Fig. 6 A_D/A_G ratio of different biochar samples derived from Raman peak fitting

well with pseudo-first-order kinetic model with $R^2 = 0.9701$ (at AB@ZnO). It is also very clear that there is a 6.6-fold enhancement in the rate of reaction of oxidative degradation for MG after adding the catalysts (AB@ZnO). This could be due to the fact that present work reports on the advance oxidation process to mineralize the dye, based on the principle of oxidation and degradation. First step is the production of hydroxyl radical, which attacks the pollutant and degrades them into simpler forms. This process is facilitated by heterogeneous catalyst such as ZnO [93]. Recyclability test of AB@ZnO after 5 cycles indicates that the mineralization efficiency boosted up to 81.4%. Thus, it is found that algae biomass creates better ZnO over its surface for catalytic application as compared to other 3 biomasses used. Also, inherent Zn containing species helps in catalytic activity. The reason for differences in the catalytic behavior can be related to the ZnO shapes, size, and nature of biochar. Porosity and hydrophobicity/hydrophilicity of biomass are directly proportional to their characteristic's biochar. It has a direct

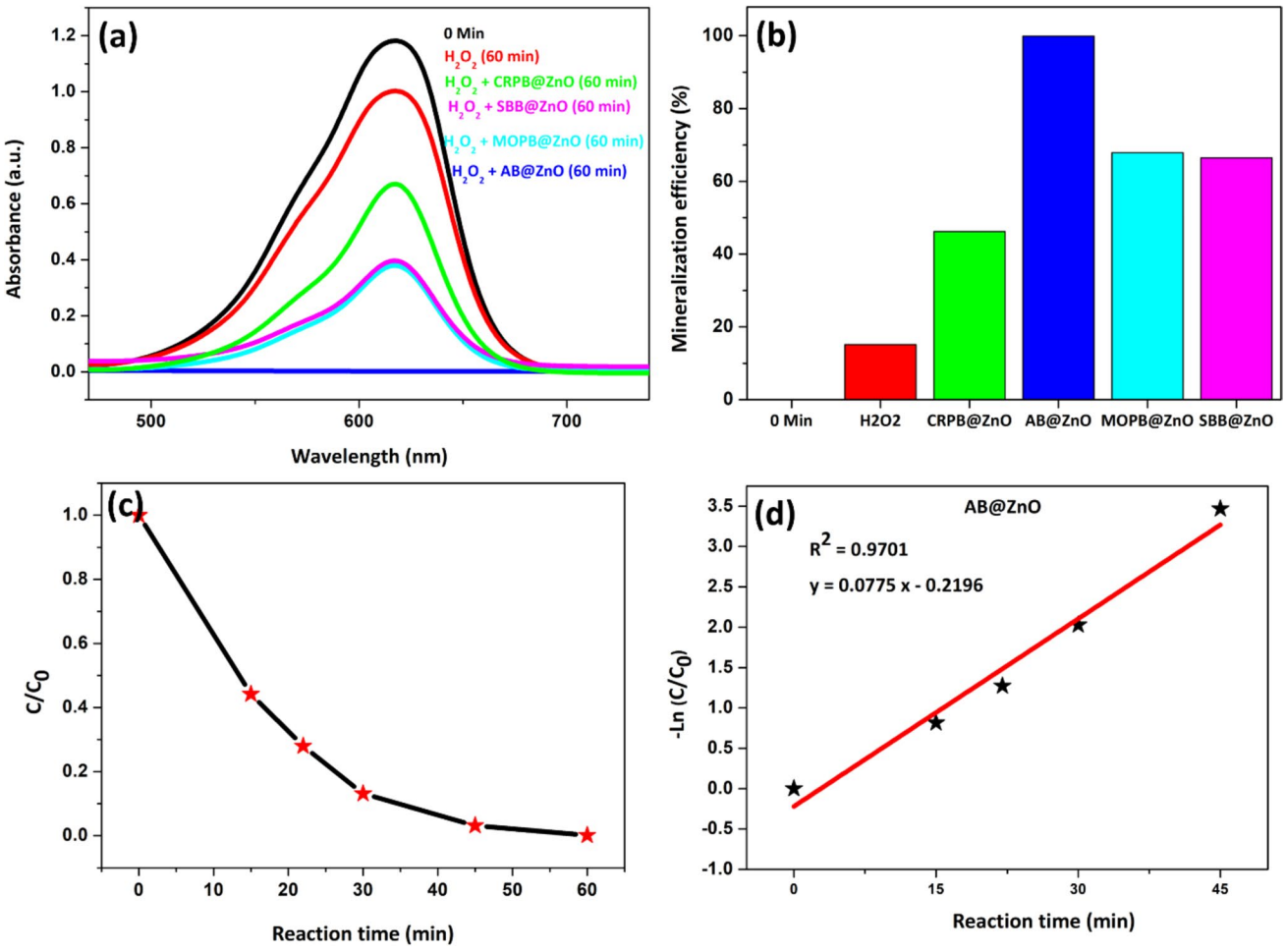

Fig. 7 **a** UV–vis spectrum of MG dye (50 ppm, 10 mL) after treatment with H_2O_2 and various catalysts, **b** corresponding mineralization efficiency of H_2O_2 and their combination (H_2O_2 + CRPB@ZnO, H_2O_2 + AB@ZnO, H_2O_2 + MOPB@ZnO, and H_2O_2 + SBB@ZnO) with various catalyst, and **c** plot of C/C_0 vs time at AB@ZnO (left side) and kinetic study (right side)

effect in the pollutant degradation. More hydrophobic biomass will give rise to more hydrophobic biochar which can face dispersibility problem while performing dye degradation experiments in aqueous medium. This fact is also supported by poor catalytic behavior of rose petals biochar@ZnO than other biochar@ZnO. Nevertheless, rose petal biochar will be a very good deal to remove oil spill via adsorption due to their hydrophobic nature. On contrary, porous and hydrophilic biomass can lead to absorbing metal salt solution more efficiently by wet impregnation process which can have direct effect on loading of metal salts, and hence concentration of ZnO on biochar surface, which has reflected in their catalytic performance positively.

The mechanism of MG dye mineralization [94] is as follows:

$$ZnO + hv_{visible} \rightarrow ZnO\left(h^{+}{}_{VB} + VB + e^{-}{}_{CB}\right)$$

$$H_2O_2 + ZnO\left(e^{-}{}_{CB}\right) \rightarrow OH^{\cdot} + OH^{-} + ZnO$$

$$ZnO\left(h^{+}{}_{VB}\right) + OH^{-} \rightarrow ZnO + OH^{\cdot}$$

$$ZnO\left(e^{-}{}_{CB}\right) + O_2 \rightarrow ZnO + O_2^{\cdot}-$$

$$O_2^{\cdot}- + H^{+} \rightarrow HO_2^{\cdot}$$

$$HO_2^{\cdot} + H^{+} + ZnO\left(e^{-}{}_{CB}\right) \rightarrow H_2O_2 + ZnO$$

$$ZnO\left(h^{+}{}_{VB}\right) + H_2O \rightarrow ZnO + H^{+} + OH^{\cdot}$$

$$MG + OH^{\cdot} \rightarrow CO_2 + H_2O + NO_{3-}$$

The step-by-step degradation pathway of MG is well reported by Jing et al. through LC–MS analysis [95]. They have demonstrated that methyl group and amine group is first attacked by the reactive species followed by the benzene ring and central carbon atom and ultimately final degradation happen. Thus, literature has proved that the presence of H_2O_2 leads to mineralization of dyes through Fenton-like process. Literature have also suggested that ZnO is a good photocatalyst under UV illumination [96], but our intention here was in the normal room light (dim). In order to further understand the mechanism of the reaction, the experiment is conducted in the dark also. It is found that the complete mineralization is also observed here (Fig. 8), and there is no difference observed when it was performed in the room having a dim light. Based on this, we have given the following explanations: H_2O_2 is oxidized when exposed to air and form hydroxyl radical. In order to have this phenomenon fast, it needs a catalyst or light or both. Then, this hydroxyl radical attacks the dye to mineralize it. In the present case probably, the light is not sufficiently strong to make the difference, but it is clearly proved that the following process can happen without providing any special light condition. Literature has revealed that in the case of photocatalysis, mineralization is faster under UV light then visible light [97].

Mixture of compound analysis would have been also interesting. However, the important aspect of the paper was to investigate the effect of different biomass on the physicochemical properties of the ZnO nanaoparticles and their catalytic activity which have been achieved successfully. Indeed, the present catalyst is expected to have the potential to mineralize the dye mixtures.

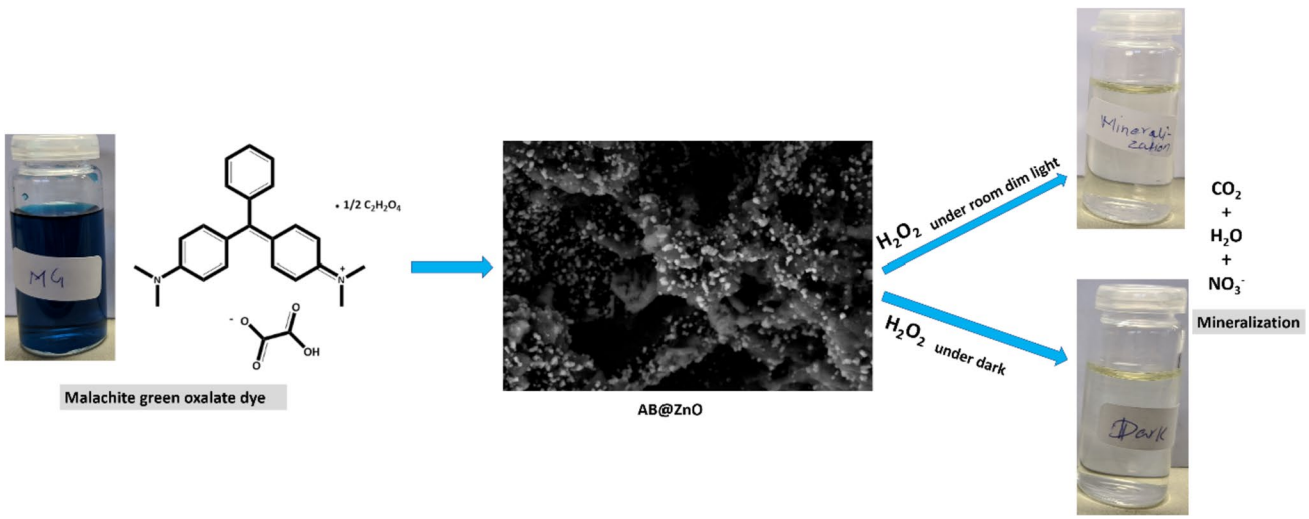

Fig. 8 MG dye (50 ppm) mineralization over AB@ZnO for 60 min under room dim light and dark

Table 4 Degradation of malachite green dye over different catalyst in the literature

Type of catalyst	Catalyst dosage	Time (min)	Temp. (°C)	H_2O_2	Conc. of MG (mg/L)	Degradation	Ref
Fe_2O_3/kaolin	800 mg/L	30	50°	7 mL	-	94.8%	[98]
Magnesium porphyrin complex (I)	5 mg	420	Room temp.	4 mL	12	84.0%	[99]
Ni/kaolin	200 mg	180	Room temp.	10 mL	20	77.8%	[100]
Fe_3O_4@SiO_2	15 mg	30	30°	50 µL	25	96.2	[101]
CRPB@ZnO	1 mg	60	Room temp.	100 µL	50	46.3%	This work
AB@ZnO	1 mg	60	Room temp.	100 µL	50	99.9%	This work
MOPB@ZnO	1 mg	60	Room temp.	100 µL	50	67.9%	This work
SBB@ZnO	1 mg	60	Room temp.	100 µL	50	66.4%	This work

When this work was compared with a reported one in literature (Table 4) for the degradation of malachite green dye, it was found that this work has advantages in terms of several parameters as mentioned below:

Cost-effectiveness: minimum catalyst dosage (just one mg) is used compared to some work where 200 mg is required.
Faster kinetics: 60 min is to mineralize the dye.
Mineralization efficiency: complete mineralization is obtained.
H_2O_2: 100 µL used but in literature, even 10 mL of H_2O_2 is used and mineralization efficiency is just 77.8%.

The above analysis has clearly proven that biochar@ZnO catalyst is very efficient in malachite green dye degradation. It is expected to have a similar effect for other pollutants. So, biochar@ZnO catalyst can play a major in the field of environmental remediation, specially the one at AB@ZnO.

4 Conclusions

Simple, cost-effective, non-toxic biochar-supported ZnO nano-catalysts have been prepared by wet impregnation of four biomasses with zinc acetate followed by pyrolysis at 500 °C under N_2 atmosphere. It is experimentally found that size, shape, and crystallinity of the nanoparticles are directly affected by their respective supports. These features are demonstrated by employing different biomass sources. The effectiveness of the catalyst is clearly proved by efficient total mineralization of malachite green dye with fast kinetics, i.e., within 60 min. It is clear that there is a 6.6-fold enhancement in the rate of reaction for the oxidative degradation of MG after adding the catalysts. This work is a step towards biomass waste valorization for sustainable development and circular bioeconomy. This simple and cost-effective process of making biochar@ZnO composite could be applied to several kinds of agrowastes and opens up an interesting perspective in the field of materials for environmental remediation. This could act as a general approach for making ZnO nanoparticle impregnation on biochar.

Apart from managing the tremendous amounts of agrowastes, biomass thermochemical conversion into biochar-based functional material is considered as a smart and cost-effective solution for a green and sustainable environmental chemistry.

Acknowledgements A.M.K. and M.M.C. would like to thank the French Government for funding AMK's contribution through a fellowship granted by the French Embassy in Egypt (Institut Français d'Egypte). We thank all the technical officers of ITODYS for XPS, Raman, XRD, and FESEM analysis. We are also grateful to ETS Laurent Mace (Huitres Creuses de Normandie, F-50560 Gouville-Sur-Mer) for providing algae samples.

Author contribution All authors contributed to the study conception and design. Material preparation, data collection, and analysis were performed by Arvind Kumar Bhakta, Mengqi Tang, Youssef Snoussi, and Mohamed Mehdi Chehimi. The first draft of the manuscript was written by Arvind Kumar Bhakta, and all authors commented on previous versions of the manuscript. All authors read and approved the final manuscript.

Funding This work was supported through "Bourse Wallonie-Bruxelles International Excellence World (no. of imputation 101386 and Article Budgetair 33.01.00.07)" and also funded by French Ministry of Research, ANR (*Agence Nationale de la Recherche) and CGI (Commissariat à l'Investissement d'Avenir) via Labex SEAM (ANR-11-LABX-086, ANR-11-IDEX-0502) grant.*

Data availability Data available upon request.

Declarations

Conflict of interest The authors declare no competing interest.

References

1. J.T. Chang, E.H. Kaplan, Modeling local coronavirus outbreaks. Eur. J. Oper. Res. **304**, 57–68 (2023). https://doi.org/10.1016/j.ejor.2021.07.049
2. A. Maruotti, D. Böhning, I. Rocchetti, M. Ciccozzi, Estimating the undetected infections in the Monkeypox outbreak, J. Med. Virol. 1–4 (2022) https://doi.org/10.1002/jmv.28099
3. H. Simon, A. Echter, Comeback of the Inflation Specter. Beating Inflat. **2023**, 1–7 (2023). https://doi.org/10.1007/978-3-031-20093-9_1
4. B. Bruckner, K. Hubacek, Y. Shan, H. Zhong, K. Feng, Impacts of poverty alleviation on national and global carbon emissions. Nat. Sustain. **5**, 311–320 (2022). https://doi.org/10.1038/s41893-021-00842-z
5. H. Pathak, Impact, adaptation, and mitigation of climate change in Indian agriculture. Environ. Monit. Assess. **195**, 52 (2023). https://doi.org/10.1007/s10661-022-10537-3
6. R. Sharma, R. Kumar, D.K. Sharma, M. Sarkar, B.K. Mishra, V. Puri, I. Priyadarshini, P.H. Thong, P.T.T. Ngo, V.-H. Nhu, Water pollution examination through quality analysis of different rivers: a case study in India. Environ. Dev. Sustain. **24**, 7471–7492 (2022). https://doi.org/10.1007/s10668-021-01777-3
7. U.K. Mishra, V.S. Chandel, O.P. Singh, A review on cerium oxide–based catalysts for the removal of contaminants. Emergent Mater. **5**, 1443–1476 (2022). https://doi.org/10.1007/s42247-021-00295-2
8. X.Y. Zhou, G. Lu, Z. Xu, X. Yan, S.T. Khu, J. Yang, J. Zhao, Influence of Russia-Ukraine War on the global energy and food security. Resour. Conserv. Recycl. **188**, 106657 (2023). https://doi.org/10.1016/j.resconrec.2022.106657
9. A. Mukherjee, N. Goswami, D. Dhak, Photocatalytic remediation of industrial dye waste streams using biochar and metal-biochar hybrids: a critical review. Chem. Africa. (2022). https://doi.org/10.1007/s42250-022-00467-5
10. M. Benjelloun, Y. Miyah, R. Bouslamti, L. Nahali, F. Mejbar, S. Lairini, The fast-efficient adsorption process of the toxic dye onto shells powders of walnut and peanut: experiments, equilibrium, thermodynamic, and regeneration studies. Chem. Africa. **5**, 375–393 (2022)
11. J. Sharma, S. Sharma, V. Soni, Toxicity of malachite green on plants and its phytoremediation: a review. Reg. Stud. Mar. Sci. **62**, 102911 (2023). https://doi.org/10.1016/j.rsma.2023.102911
12. J. Song, G. Han, Y. Wang, X. Jiang, D. Zhao, M. Li, Y. Zhen, M. Qingyun, R.E. Parales, R. Zhiyong, Y. Mu, Pathway and kinetics of malachite green biodegradation by Pseudomonas veronii. Sci. Rep. **10**, 4502 (2020). https://doi.org/10.1038/s41598-020-61442-z
13. D. Pandey, A. Daverey, K. Dutta, K. Arunachalam, Bioremoval of toxic malachite green from water through simultaneous decolorization and degradation using laccase immobilized biochar. Chemosphere **297**, 134126 (2022). https://doi.org/10.1016/j.chemosphere.2022.134126
14. P.O. Oladoye, T.O. Ajiboye, W.C. Wanyonyi, E.E.O. Omotola, M.E. Oladipo, Insights into remediation technology for malachite green wastewater treatment. Water Sci. Eng. **16**, 261–270 (2023). https://doi.org/10.1016/j.wse.2023.03.002
15. S. Lahan, R. Kant, Investigating the sustainable development goals derived due to adoption of circular economy practices. Waste Manag. **143**, 1–14 (2022). https://doi.org/10.1016/j.wasman.2022.02.016
16. M. Nematian, C. Keske, J.N. Ng'ombe, A techno-economic analysis of biochar production and the bioeconomy for orchard biomass. Waste Manag. **135**, 467–477 (2021). https://doi.org/10.1016/j.wasman.2021.09.014
17. S. Pap, K.G. Boyd, M.A. Taggart, M. Turk Sekulic, Circular economy based landfill leachate treatment with sulphur-doped microporous biochar. Waste Manag. **124**, 160–171 (2021). https://doi.org/10.1016/j.wasman.2021.01.037
18. A.K. Bhakta, Y. Snoussi, M. El Garah, S. Ammar, M.M. Chehimi, Brewer's spent grain biochar : grinding method matters. J. Carbon Res. **8**, 46 (2022). https://doi.org/10.3390/c8030046
19. G.F. Ghesti, E.A. Silveira, M.G. Guimarães, R.B.W. Evaristo, M. Costa, Towards a sustainable waste-to-energy pathway to pequi biomass residues: biochar, syngas, and biodiesel analysis. Waste Manag. **143**, 144–156 (2022). https://doi.org/10.1016/j.wasman.2022.02.022
20. M. Gęca, A.M. Khalil, M. Tang, A.K. Bhakta, Y. Snoussi, P. Nowicki, M. Wiśniewska, M.M. Chehimi, Surface treatment of biochar—methods, surface analysis and potential applications: a comprehensive review. Surfaces. **6**, 179–213 (2023). https://doi.org/10.3390/surfaces6020013
21. V. Shanmugam, S.N. Sreenivasan, R.A. Mensah, M. Försth, G. Sas, M.S. Hedenqvist, R.E. Neisiany, Y. Tu, O. Das, A review on combustion and mechanical behaviour of pyrolysis biochar. Mater. Today Commun. **31**, 103629 (2022). https://doi.org/10.1016/j.mtcomm.2022.103629
22. C. Pandit, S. Pandit, M. Pant, D. Ghosh, D. Agarwal, D. Lahiri, M. Nag, R.R. Ray, A concise review on the synthesis, and characterization of the pyrolytic lignocellulosic biomass for oil, char and gas production: recent advances and its environmental application. Chem. Africa. (2022). https://doi.org/10.1007/s42250-022-00512-3
23. S. Greenough, M.-J. Dumont, S. Prasher, The physicochemical properties of biochar and its applicability as a filler in rubber composites : a review. Mater. Today Commun. **29**, 102912 (2021). https://doi.org/10.1016/j.mtcomm.2021.102912
24. K. Weber, P. Quicker, Properties of biochar. Fuel **217**, 240–261 (2018). https://doi.org/10.1016/j.fuel.2017.12.054
25. A.K. Bhakta, R. Fiorenza, K. Jlassi, Z. Mekhalif, A.M.A. Ali, M.M. Chehimi, The emerging role of biochar in the carbon materials family for hydrogen production. Chem. Eng. Res. Des. **188**, 209–228 (2022). https://doi.org/10.1016/j.cherd.2022.09.028
26. A. Saravanan, P.S. Kumar, Biochar derived carbonaceous material for various environmental applications: systematic review. Environ. Res. **214**, 113857 (2022). https://doi.org/10.1016/j.envres.2022.113857
27. M.M. Jacob, M. Ponnuchamy, A. Kapoor, P. Sivaraman, Adsorptive decontamination of organophosphate pesticide chlorpyrifos from aqueous systems using bagasse-derived biochar alginate beads : thermodynamic, equilibrium, and kinetic studies. Chem. Eng. Res. Des. **186**, 241–251 (2022). https://doi.org/10.1016/j.cherd.2022.07.043
28. Z. Chen, V. Kamchoom, A. Apriyono, R. Chen, C. Chen, Laboratory study of water infiltration and evaporation in biochar-amended landfill covers under extreme climate. Waste Manag.

153, 323–334 (2022). https://doi.org/10.1016/j.wasman.2022.09.015
29. P. Choudhary, M. Prasad, M. Choudhary, A. Kumar, S. Kumar, R. Srinivasan, S.K. Mahawer, Exploring invasive weed biochar as soil amendment: a study on fodder oats productivity and soil biological properties. Environ. Res. **216**, 114527 (2023). https://doi.org/10.1016/j.envres.2022.114527
30. A.K. Singh, Engineered biochar for oil/water separation : processing and mechanism. Bioresour. Technol. Rep. **20**, 101269 (2022). https://doi.org/10.1016/j.biteb.2022.101269
31. Y. Snoussi, I. Sifaoui, A.M. Khalil, A.K. Bhakta, O. Semyonov, P.S. Postnikov, L. Michely, R. Pires, S. Bastide, J.E.-P. Barroso, J.L. Morales, M.M. Chehimi, Facile synthesis of silver decorated biochar as a novel and highly active biosourced anti-kinetoplastid agent. Mater. Today Commun. **32**, 104126 (2022). https://doi.org/10.1016/j.mtcomm.2022.104126
32. A. Bopda, S.G.M. Mafo, J.N. Ndongmo, G.T. Kenda, C.G. Fotsop, I.T. Kuete, C.S. Ngakou, D.R.T. Tchuifon, A.K. Tamo, G.N. Nche, S.G. Anagho, Ferromagnetic biochar prepared from hydrothermally modified calcined mango seeds for Fenton-like degradation of indigo carmine. J. Carbon Res. **8**, 81 (2022). https://doi.org/10.3390/c8040081
33. L. Boubkr, A.K. Bhakta, Y. Snoussi, C.M. Da Silva, L. Michely, M. Jouini, S. Ammar, M.M. Chehimi, Highly active Ag-Cu nanocrystal catalyst-coated brewer's spent grain biochar for the mineralization of methyl orange and methylene blue dye mixture. Catalysts **12**, 1475 (2022). https://doi.org/10.3390/catal12111475
34. L.C. de Almeida, F.A. de Jesus, F.M. S.Wiltshire, R.M. Santos, A.T. Fricks, L. dos S. Freitas, M.M. Pereira, Á.S. Lima, C.M.F. Soares, Development of carbon-based support using biochar from guava seeds for lipase immobilization, C. **8**, 64 (2022) https://www.mdpi.com/2311-5629/8/4/64/htm%0Ahttps://www.mdpi.com/2311-5629/8/4/64
35. N.A.A. Mohd Azan, S. Sagadevan, A.R. Mohamed, A.H. Nor Azazi, F.B.M. Suah, T. Kobayashi, R. Adnan, N.H. MohdKaus, Solar light-induced photocatalytic degradation of ciprofloxacin antibiotic using biochar supported nano bismuth ferrite composite. Catalysts. **12**, 1269 (2022). https://doi.org/10.3390/catal12101269
36. A.A. Ioannidi, J. Vakros, Z. Frontistis, D. Mantzavinos, Tailoring the biochar physicochemical properties using a friendly ecomethod and its application on the oxidation of the drug losartan through persulfate activation. Catalyst. **12**, 1245 (2022). https://doi.org/10.3390/catal12101245
37. S.M. Badiger, P. V Nidheesh, Applications of biochar in sulfate radical-based advanced oxidation processes for the removal of pharmaceuticals and personal care products. Water Sci. Technol. (2023)https://doi.org/10.2166/wst.2023.069.
38. J. Viaene, N. Peiren, D. Vandamme, A. Lataf, A. Cuypers, M. Jozefczak, F. Amery, B. Vandecasteele, Screening tests for N sorption allow to select and engineer biochars for N mitigation during biomass processing. Waste Manag. **155**, 230–239 (2023). https://doi.org/10.1016/j.wasman.2022.10.037
39. B. Nicole, H. Macek, Y. Gariepy, M. Francis, S. Prasher, C.Y. Khripin, J.J. Mehlem, M.-J. Dumont, Evaluating corn-based biochar as an alternative to carbon black in styrene-butadiene rubber composites. Mater. Today Commun. **34**, 105218 (2023). https://doi.org/10.1016/j.mtcomm.2022.105218
40. A. Kali, A. Amar, I. Loulidi, C. Hadey, M. Jabri, A.A. Alrashdi, H. Lgaz, M. Sadoq, A. El-Kordy, F. Boukhlifi, Efficient adsorption removal of an anionic azo dye by lignocellulosic waste material and sludge recycling into combustible briquettes. Colloids Interfaces. **6**, 22 (2022). https://doi.org/10.3390/colloids6020022
41. İA. Başar, C. Eskicioglu, N.A. Perendeci, Biochar and wood ash amended anaerobic digestion of hydrothermally pretreated lignocellulosic biomass for biorefinery applications. Waste Manag. **154**, 350–360 (2022). https://doi.org/10.1016/j.wasman.2022.10.014
42. R. Castejón-del Pino, M.L. Cayuela, M. Sánchez-García, M.A. Sánchez-Monedero, Nitrogen availability in biochar-based fertilizers depending on activation treatment and nitrogen source. Waste Manag. **158**, 76–83 (2023). https://doi.org/10.1016/j.wasman.2023.01.007
43. Y. Han, D. Yue, Y. Zhao, X. Qian, Nano-Fe(0)/mesoporous carbon supported on biochar for activating peroxydisulfate to remove polycyclic aromatics hydrocarbons. Emergent Mater. **3**, 307–313 (2020). https://doi.org/10.1007/s42247-020-00100-6
44. L.C. de Almeida, E.L.O. Andrade, J.C.B. Santos, R.M. Santos, A.T. Fricks, L.S. dos Freitas, Á.S. Lima, M.M. Pereira, C.M.F. Soares, Novel nanobiocatalyst constituted by lipase from Burkholderia cepacia immobilized on graphene oxide derived from grape seed biochar. C **9**, 12 (2023). https://doi.org/10.3390/c9010012
45. S. Sutar, P. Patil, J. Jadhav, Recent advances in biochar technology for textile dyes wastewater remediation : a review. Environ. Res. **209**, 112841 (2022). https://doi.org/10.1016/j.envres.2022.112841
46. S. Anto, M.P. Sudhakar, T.S. Ahamed, M.S. Samuel, T. Mathimani, K. Brindhadevi, A. Pugazhendhi, Activation strategies for biochar to use as an efficient catalyst in various applications. Fuel **285**, 119205 (2021). https://doi.org/10.1016/j.fuel.2020.119205
47 E. KhoshnoodMotlagh, S. Sharifian, N. Asasian-Kolur, Alkaline activating agents for activation of rice husk biochar and simultaneous bio-silica extraction. Bioresour. Technol. Rep. **16**, 100853 (2021). https://doi.org/10.1016/j.biteb.2021.100853
48. J. Omiri, Y. Snoussi, A.K. Bhakta, S. Truong, S. Ammar, A.M. Khalil, M. Jouini, M.M. Chehimi, Citric-acid-assisted preparation of biochar loaded with copper / nickel bimetallic nanoparticles for dye degradation. Colloids Interfaces. **6**, 18 (2022). https://doi.org/10.3390/colloids6020018
49. B. Sajjadi, W.Y. Chen, N.O. Egiebor, A comprehensive review on physical activation of biochar for energy and environmental applications. Rev. Chem. Eng. **35**, 735–776 (2019). https://doi.org/10.1515/revce-2017-0113
50. Y. Al-Douri, ZnO nanostructures: analysis and characterization by the electrospinning technique. Emergent Mater. **3**, 947–953 (2020). https://doi.org/10.1007/s42247-020-00144-8
51. S. Samreen, D. Devadiga, B.M. Samrudhi, T.N. Ahipa, K.K. Sadasivuni, Synthesis and mechanochromic investigations of new cyanopyridone derivatives. Dye. Pigment. **211**, 111080 (2023). https://doi.org/10.1016/j.dyepig.2023.111080
52. I. Dhahri, M. Ellouze, S. Labidi, Q.M. Al-Bataineh, J. Etzkorn, H. Guermazi, A. Telfah, C.J. Tavares, R. Hergenröder, T. Appel, Optical and structural properties of ZnO NPs and ZnO–Bi2O3 nanocomposites. Ceram. Int. **48**, 266–277 (2022). https://doi.org/10.1016/j.ceramint.2021.09.101
53. P. Kumari, A. Srivastava, R.K. Sharma, A. Saini, D. Sharma, J.S. Tawale, S.K. Srivastava, Facile synthesis and tailoring the structural and photoluminescence properties of ZnO nanoparticles via annealing in air atmosphere. Mater. Today Commun. **32**, 103845 (2022). https://doi.org/10.1016/j.mtcomm.2022.103845
54. E.E. Elemike, D.C. Onwudiwe, J.I. Mbonu, Facile synthesis of cellulose–ZnO-hybrid nanocomposite using Hibiscus rosa-sinensis leaf extract and their antibacterial activities. Appl. Nanosci. **11**, 1349–1358 (2021). https://doi.org/10.1007/s13204-021-01774-y
55. D. Bhuyan, B. Malakar, S.S. Arbuj, L. Saikia, Flower shaped homocentric pencil like ZnO nanorod bundles: synthesis, characterisation and study of their photocatalytic activity. RSC Adv. **4**, 8256–8259 (2014). https://doi.org/10.1039/c3ra45818k
56 S. Selvamani, S. Balamurugan, S.A. Ashika, T.K.S. Fathima, The remarkable enhancement in the solubility of Bi in the ZnO phase,

Zn1-xBixO ($0 \leq x \leq 0.1$), by high energy ball milling technique. Emergent Mater. **4**, 1399–1411 (2021). https://doi.org/10.1007/s42247-021-00286-3
57. L.M. Mahlaule-Glory, N.C. Hintsho-Mbita, Green derived zinc oxide (ZnO) for the degradation of dyes from wastewater and their antimicrobial activity: a review. Catalysts **12**, 833 (2022). https://doi.org/10.3390/catal12080833
58. A.R. Bhapkar, M. Geetha, D. Jaspal, K. Gheisari, M. Laad, J.J. Cabibihan, K.K. Sadasivuni, S. Bhame, Aluminium doped ZnO nanostructures for efficient photodegradation of indigo carmine and azo carmine G in solar irradiation. Appl. Nanosci. **13**, 5777–5793 (2023). https://doi.org/10.1007/s13204-023-02824-3
59. V. Vinitha, M. Preeyanghaa, V. Vinesh, R. Dhanalakshmi, B. Neppolian, V. Sivamurugan, Two is better than one: catalytic, sensing and optical applications of doped zinc oxide nanostructures. Emergent Mater. **4**, 1093–1124 (2021). https://doi.org/10.1007/s42247-021-00262-x
60. F. Güell, A. Galdámez-Martínez, P.R. Martínez-Alanis, A.C. Catto, L.F. da Silva, V.R. Mastelaro, G. Santana, A. Dutt, ZnO-based nanomaterials approach for photocatalytic and sensing applications: recent progress and trends. Mater. Adv. **4**, 3685–3707 (2023). https://doi.org/10.1039/d3ma00227f
61. H. Mankomal, Kaur, Synergistic effect of biochar impregnated with ZnO nano-flowers for effective removal of organic pollutants from wastewater. Appl. Surf. Sci. Adv. **12**, 100339 (2022). https://doi.org/10.1016/j.apsadv.2022.100339
62. Y.A.E.H. Ali, M. Ahrouch, A.A. Lahcen, Y. Abdellaoui, M. Stitou, Recent advances and prospects of biochar-based adsorbents for malachite green removal: a comprehensive review. Chem. Africa. (2022). https://doi.org/10.1007/s42250-022-00391-8
63. A. Saravanan, V.C. Deivayanai, P.S. Kumar, G. Rangasamy, R.V. Hemavathy, T. Harshana, N. Gayathri, K. Alagumalai, A detailed review on advanced oxidation process in treatment of wastewater: mechanism, challenges and future outlook. Chemosphere **308**, 136524 (2022). https://doi.org/10.1016/j.chemosphere.2022.136524
64. J.A. Garrido-Cardenas, B. Esteban-García, A. Agüera, J.A. Sánchez-Pérez, F. Manzano-Agugliaro, Wastewater treatment by advanced oxidation process and their worldwide research trends. Int. J. Environ. Res. Public Health **17**, 170 (2020). https://doi.org/10.3390/ijerph17010170
65. H. Bayoka, Y. Snoussi, A.K. Bhakta, M. El Garah, A.M. Khalil, M. Jouini, S. Ammar, M.M. Chehimi, Evidencing the synergistic effects of carbonization temperature, surface composition and structural properties on the catalytic activity of biochar/bimetallic composite. J. Anal. Appl. Pyrolysis **173**, 106069 (2023). https://doi.org/10.1016/j.jaap.2023.106069
66. P.V. Nidheesh, S.O. Ganiyu, C.A. Martínez-Huitle, E. Mousset, H. Olvera-Vargas, C. Trellu, M. Zhou, M.A. Oturan, Recent advances in electro-Fenton process and its emerging applications. Crit. Rev. Environ. Sci. Technol. 53 (2023) https://doi.org/10.1080/10643389.2022.2093074
67 K.D. Gonzalez-Gloria, R.M. Rodríguez-Jasso, Shiva, E. Aparicio, M.L.C. Gonzalez, E.T. Kostas, H.A. Ruiz, Macroalgal biomass in terms of third-generation biorefinery concept : current status and techno-economic analysis—a review. Bioresour. Technol. Rep. **16**, 100863 (2021). https://doi.org/10.1016/j.biteb.2021.100863
68. J. Leichtweis, S. Silvestri, E. Carissimi, New composite of pecan nutshells biochar-ZnO for sequential removal of acid red 97 by adsorption and photocatalysis. Biomass Bioenerg. **140**, 105648 (2020). https://doi.org/10.1016/j.biombioe.2020.105648
69. Y. He, Y. Wang, J. Hu, K. Wang, Y. Zhai, Y. Chen, Y. Duan, Y. Wang, W. Zhang, Photocatalytic property correlated with microstructural evolution of the biochar/ZnO composites. J. Mater. Res. Technol. **11**, 1308–1321 (2021). https://doi.org/10.1016/j.jmrt.2021.01.077
70. M. Amir, T. Fazal, J. Iqbal, A.A. Din, A. Ahmed, A. Ali, A. Razzaq, Z. Ali, M.S.U. Rehman, Y.K. Park, Integrated adsorptive and photocatalytic degradation of pharmaceutical micropollutant, ciprofloxacin employing biochar-ZnO composite photocatalysts. J. Ind. Eng. Chem. **115**, 171–182 (2022). https://doi.org/10.1016/j.jiec.2022.07.050
71. A. Kamal, M.H. Saleem, H. Alshaya, M.K. Okla, H.J. Chaudhary, M.F.H. Munis, Ball-milled synthesis of maize biochar-ZnO nanocomposite (MB-ZnO) and estimation of its photocatalytic ability against different organic and inorganic pollutants. J. Saudi Chem. Soc. **26**, 101445 (2022). https://doi.org/10.1016/j.jscs.2022.101445
72. N.P.F. Gonçalves, M.A.O. Lourenço, S.R. Baleuri, S. Bianco, P. Jagdale, P. Calza, Biochar waste-based ZnO materials as highly efficient photocatalysts for water treatment. J. Environ. Chem. Eng. **10**, 107256 (2022). https://doi.org/10.1016/j.jece.2022.107256
73. J. Fito, K.K. Kefeni, T.T.I. Nkambule, The potential of biochar-photocatalytic nanocomposites for removal of organic micropollutants from wastewater. Sci. Total. Environ. **829**, 154648 (2022). https://doi.org/10.1016/j.scitotenv.2022.154648
74. E. Weidner, E. Karbassiyazdi, A. Altaee, T. Jesionowski, F. Ciesielczyk, Hybrid metal oxide/biochar materials for wastewater treatment technology: a review. ACS Omega **7**, 27062–27078 (2022). https://doi.org/10.1021/acsomega.2c02909
75. C. Zhao, B. Wang, B.K.G. Theng, P. Wu, F. Liu, S. Wang, X. Lee, M. Chen, L. Li, X. Zhang, Formation and mechanisms of nano-metal oxide-biochar composites for pollutants removal: a review. Sci. Total. Environ. **767**, 145305 (2021). https://doi.org/10.1016/j.scitotenv.2021.145305
76. A. Fleming, R.M. Wise, H. Hansen, L. Sams, The sustainable development goals: a case study. Mar. Policy **86**, 94–103 (2017). https://doi.org/10.1016/j.marpol.2017.09.019
77. A.M. Khalil, L. Michely, R. Pires, S. Bastide, K. Jlassi, S. Ammar, M. Jaziri, M.M. Chehimi, Copper/nickel-decorated olive pit biochar: one pot solid state synthesis for environmental remediation. Appl. Sci. **11**, 8513 (2021). https://doi.org/10.3390/app11188513
78. H. Bamdad, S. Papari, E. Moreside, F. Berruti, High-temperature pyrolysis for elimination of per- and polyfluoroalkyl substances (PFAS) from biosolids. Processes. **10**, 2187 (2022). https://doi.org/10.3390/pr10112187
79. S. Kundu, S. Patel, P. Halder, T. Patel, M. HedayatiMarzbali, B.K. Pramanik, J. Paz-Ferreiro, C.C. De Figueiredo, D. Bergmann, A. Surapaneni, M. Megharaj, K. Shah, Removal of PFASs from biosolids using a semi-pilot scale pyrolysis reactor and the application of biosolids derived biochar for the removal of PFASs from contaminated water. Environ. Sci. Water Res. Technol. **7**, 638–649 (2021). https://doi.org/10.1039/d0ew00763c
80. E. Zanchetta, E. Damergi, B. Patel, T. Borgmeyer, H. Pick, A. Pulgarin, C. Ludwig, Algal cellulose, production and potential use in plastics: challenges and opportunities. Algal Res. **56**, 102288 (2021). https://doi.org/10.1016/j.algal.2021.102288
81. S. Wan, Y. Li, S. Cheng, G. Wu, X. Yang, Y. Wang, L. Gao, Cadmium removal by FeOOH nanoparticles accommodated in biochar : 4ffect of the negatively charged functional groups in host. J. Hazard. Mater. **421**, 126807 (2022). https://doi.org/10.1016/j.jhazmat.2021.126807
82. W. Ahmed, S. Mehmood, M. Mahmood, S. Ali, A. Shakoor, A. Núñez-Delgado, R.M.A. Asghar, H. Zhao, W. Liu, W. Li, Adsorption of Pb(II) from wastewater using a red mud modified rice-straw biochar: Influencing factors and reusability. Environ.

Pollut. **326**, 121405 (2023). https://doi.org/10.1016/j.envpol.2023.121405
83. J. Albertsson, S.C. Abrahams, Å. Kvick, Atomic displacement, anharmonic thermal vibration, expansivity and pyroelectric coefficient thermal dependences in ZnO. Acta Crystallogr. Sect. B. **45**, 34–40 (1989). https://doi.org/10.1107/S0108768188010109
84. G. Donnay, K. Kihara, Powder Diffr. 1 (1986) 64–77
85. H. Schulz, K.H. Thiemann, Structure parameters and polarity of the wurtzite type compounds Sic—2H and ZnO. Solid State Commun. **32**, 783–785 (1979). https://doi.org/10.1016/0038-1098(79)90754-3
86. Y. Yoshizawa, A. Ametani, J. Tsunehiro, K. Nomura, M. Itoh, F. Fukui, S. Kaminogawa, Macrophage stimulation activity of the polysaccharide fraction from a marine alga (Porphyra yezoensis): structure-function relationships and improved solubility. Biosci. Biotechnol. Biochem. **59**, 1933–1937 (1995). https://doi.org/10.1271/bbb.59.1933
87. S. Bera, S. Dhara, S. Velmurugan, A.K. Tyagi, Analysis on binding energy and Auger parameter for estimating size and stoichiometry of ZnO nanorods. Int. J. Spectrosc. **2012**, 1–4 (2012). https://doi.org/10.1155/2012/371092
88 P. Binnal, D.J. Kumar, M. SasaluParameshwaraiah, J. Patil, Upgrading rice husk biochar characteristics through microwave-assisted phosphoric acid pretreatment followed by co-pyrolysis with LDPE. Biofuels Bioprod. Biorefining. **16**, 1254–1273 (2022). https://doi.org/10.1002/bbb.2392
89. S. Patel, M. HedayatiMarzbali, I.G. Hakeem, G. Veluswamy, N. Rathnayake, K. Nahar, S. Agnihotri, D. Bergmann, A. Surapaneni, R. Gupta, A. Sharma, K. Shah, Production of H2 and CNM from biogas decomposition using biosolids-derived biochar and the application of the CNM-coated biochar for PFAS adsorption. Waste Manag. **159**, 146–153 (2023). https://doi.org/10.1016/j.wasman.2023.01.037
90. V. Dodevski, B. Janković, I. Radović, M. Stojmenović, M. Čebela, Ž Nikolić, M.C. Pagnacco, I. Panić, M. Stanković, Characterization analysis of activated carbon derived from the carbonization process of plane tree (Platanus orientalis) seeds. Energy Environ. **31**, 583–612 (2020). https://doi.org/10.1177/0958305X19880878
91. Y. Wu, Y. Sun, K. Liang, Z. Yang, R. Tu, X. Fan, S. Cheng, H. Yu, E. Jiang, X. Xu, Enhancing hydrodeoxygenation of bio-oil via bimetallic Ni-V catalysts modified by cross-surface migrated-carbon from biochar. ACS Appl. Mater. Interfaces **13**, 21482–21498 (2021). https://doi.org/10.1021/acsami.1c05350
92. S.T. Neeli, H. Ramsurn, Synthesis and formation mechanism of iron nanoparticles in graphitized carbon matrix using biochar from biomass model compounds as a support. Carbon N. Y. **134**, 480–490 (2018). https://doi.org/10.1016/j.carbon.2018.03.079
93. M. Malakootian, A. Nasiri, A.N. Alibeigi, H. Mahdizadeh, M.A. Gharaghani, Synthesis and stabilization of ZnO nanoparticles on a glass plate to study the removal efficiency of acid red 18 by hybrid advanced oxidation process (ultraviolet / ZnO / ultrasonic). Desalin. Water Treat. **170**, 325–336 (2019). https://doi.org/10.5004/dwt.2019.24728
94. B. Pare, V.S. Barde, V.S. Solanki, N. Agarwal, V.K. Yadav, M.M. Alam, A. Gacem, T. Alsufyani, N. Ben Khedher, J.-W. Park, S. Park, B.-H. Jeon, Green synthesis and characterization of LED-irradiation- responsive nano ZnO catalyst and photocatalytic mineralization of malachite green dye. Water **14**, 3221 (2022). https://doi.org/10.3390/w14203221
95. H. Jing, L. Ji, Z. Wang, J. Guo, S. Lu, J. Sun, L. Cai, Y. Wang, Synthesis of ZnO nanoparticles loaded on biochar derived from spartina alterniflora with superior photocatalytic degradation performance. Nanomaterials **11**, 2479 (2021). https://doi.org/10.3390/nano11102479
96. R. Haounati, H. Ighnih, R.E. Malekshah, S. Alahiane, F. Alakhras, E. Alabbad, H. Alghamdi, H. Ouachtak, A.A. Addi, A. Jada, Exploring ZnO/Montmorillonite photocatalysts for the removal of hazardous RhB dye: a combined study using molecular dynamics simulations and experiments. Mater. Today Commun. **35**, 105915 (2023). https://doi.org/10.1016/j.mtcomm.2023.105915
97 V. Lakshmi Prasanna, V. Rajagopalan, A new synergetic nanocomposite for dye degradation in dark and light. Sci. Rep. **6**, 38606 (2016). https://doi.org/10.1038/srep38606
98. A. Bellal, Wet hydrogen peroxide catalytic oxidation of malachite green over Fe2O3 / Kaolin catalyst : optimization of reaction parameters. Int. J. Eng. Res. Dev. **17**, 01–07 (2021)
99. K. Ezzayani, A. Ben Khelifa, A. Guesmi, N. Ben Hamadi, A. Houas, H. Nasri., Adsorption and catalytic degradation of malachite green by a new magnesium porphyrin complex. SSRN. Prepr. 1–21 (2022)
100. A. Moumen, Y. Belhocine, N. Sbei, S. Rahali, F.A.M. Ali, F. Mechati, F. Hamdaoui, M. Seydou, Removal of malachite green dye from aqueous solution by catalytic wet oxidation technique using Ni/kaolin as catalyst. Molecules **27**, 7528 (2022). https://doi.org/10.3390/molecules27217528
101. N. Mahmud, A. Benamor, M.S. Nasser, M.M. Ba-Abbad, M.H. El-Naas, A.W. Mohammad, Effective heterogeneous Fenton-like degradation of malachite green dye using the core-shell Fe3O4@SiO2 nano-catalyst. ChemistrySelect **6**, 865–875 (2021). https://doi.org/10.1002/slct.202003937